

Article

Stone Fruit Seed: A Source of Renewable Fuel for Transport

M. Anwar ¹, M. G. Rasul ¹, N. M. S. Hassan ^{2,*}, M. I. Jahirul ¹, Rezwanul Haque ³, M. M. Hasan ¹,
A. G. M. B. Mustayen ⁴, R. Karami ⁵ and D. Schaller ⁶

¹ School of Engineering and Technology, Central Queensland University, Rockhampton, QLD 4701, Australia; m.anwar@cqu.edu.au (M.A.); m.rasul@cqu.edu.au (M.G.R.); m.j.islam@cqu.edu.au (M.I.J.); m.m.hasan@cqu.edu.au (M.M.H.)

² School of Engineering and Technology, Central Queensland University, Cairns, QLD 4870, Australia

³ School of Science, Technology and Engineering, University of the Sunshine Coast, Sippy Downs, QLD 4556, Australia; rhaque@usc.edu.au

⁴ School of Engineering, University of Tasmania, Hobart, TAS 7001, Australia; agmmustayen.billah@utas.edu.au

⁵ Oil and Gas Research Center (OGRC), Persian Gulf University, Bushehr 7516913817, Iran; karami.rahim@gmail.com

⁶ Southern Oil Refineries, Gladstone, QLD 4694, Australia; schallad@gmail.com

* Correspondence: n.hassan@cqu.edu.au

Abstract: This study investigated the suitability of stone fruit seed as a source of biodiesel for transport. Stone fruit oil (SFO) was extracted from the seed and converted into biodiesel. The biodiesel yield of 95.75% was produced using the alkaline catalysed transesterification process with a methanol-to-oil molar ratio of 6:1, KOH catalyst concentration of 0.5 wt% (weight %), and a reaction temperature of 55 °C for 60 min. The physicochemical properties of the produced biodiesel were determined and found to be the closest match of standard diesel. The engine performance, emissions and combustion behaviour of a four-cylinder diesel engine fuelled with SFO biodiesel blends of 5%, 10% and 20% with diesel, *v/v* basis, were tested. The testing was performed at 100% engine load with speed ranging from 200 to 2400 rpm. The average brake specific fuel consumption and brake thermal efficiency of SFO blends were found to be 4.7% to 15.4% higher and 3.9% to 11.4% lower than those of diesel, respectively. The results also revealed that SFO biodiesel blends have marginally lower in-cylinder pressure and a higher heat release rate compared to diesel. The mass fraction burned results of SFO biodiesel blends were found to be slightly faster than those of diesel. The SFO biodiesel 5% blend produced about 1.9% higher NO_x emissions and 17.4% lower unburnt HC with 23.4% lower particulate matter (PM) compared to diesel fuel. To summarise, SFO biodiesel blends are recommended as a suitable transport fuel for addressing engine emissions problems and improving combustion performance with a marginal sacrifice of engine efficiency.

Keywords: stone fruit; apricot; binary; combustion; emissions; diesel engine; biodiesel; transesterification; and particulate matter emission



Citation: Anwar, M.; Rasul, M.G.; Hassan, N.M.S.; Jahirul, M.I.; Haque, R.; Hasan, M.M.; Mustayen, A.G.M.B.; Karami, R.; Schaller, D. Stone Fruit Seed: A Source of Renewable Fuel for Transport. *Energies* **2022**, *15*, 4667. <https://doi.org/10.3390/en15134667>

Academic Editor: Attilio Converti

Received: 21 April 2022

Accepted: 22 June 2022

Published: 25 June 2022

Publisher's Note: MDPI stays neutral with regard to jurisdictional claims in published maps and institutional affiliations.



Copyright: © 2022 by the authors. Licensee MDPI, Basel, Switzerland. This article is an open access article distributed under the terms and conditions of the Creative Commons Attribution (CC BY) license (<https://creativecommons.org/licenses/by/4.0/>).

1. Introduction

Energy has become an indispensable factor for human survival and economic development since the beginning of the technological revolution of the late 18th and early 19th centuries. Global demand for primary oil will rise by 1.2 percent annually between 2017 and 2040, requiring an additional 32% capacity to meet this need [1]. Nevertheless, the main energy sources can be categorised into three types: fossil, fissile and renewable. Fossil energy sources develop over a long period of time and are not renewable. Plutonium and thorium are the primary fissile energy source materials that can be broken into zero kinetic energy neutrons. Renewable energy is derived from natural sources, including biomass, solar, air, wind, geothermal, marine and hydrogen energy sources. Fossil energy is the largest single energy source, fulfilling 88% of the world's total energy demand, whereas renewable

energy sources represent only 5% [2]. However, considering the current consumption rate, fossil energy is depleting rapidly and cannot be replaced because of its non-renewable nature. It is also largely responsible for producing harmful pollutants and contributing to global warming. Moreover, CO₂ emissions from energy consumption are expected to rise to almost 10% by the year 2040 [1]. The creation of sustainable, alternative, non-fossil-based energy sources is therefore paramount given the current energy scenario and to ensure that energy consumption needs and environmental challenges are met well into the future. As a consequence, the uses of alternative energy sources, including biofuels [3–7], solar [8–10], wind [11,12] and hydrogen [13,14], are increasing; these are not only renewable but also offer many socio-economic advantages over conventional fossil energy.

Biodiesel is a type of biofuel that has gained enormous global attention in recent decades as a renewable alternative to fossil-based fuels. It is a diesel-like fuel obtained from biomass-based bio-oil, vegetable oil or animal fat feedstock through the transesterification chemical process, which is required to meet the quality parameters of international biodiesel standards [15,16]. It can be used directly in conventional diesel engines without requiring any engine modification and also offers many benefits over fossil diesel. Some of the main benefits of using biodiesel are its safe, organic, non-toxic and biodegradable nature, and that it is a more effective lubricant, prolonging the life of the engine through the reduction in wear and tear of moving engine parts [17]. Biodiesels are biodegradable and cause little environmental pollution even during accidental spillage. They can significantly reduce unburned carbon monoxides, particulate matter, hydrocarbons, and sulphur dioxide emissions compared to petroleum diesel when running in the same engine. Particulate matter in biodiesel exhaust emissions is around 30% less compared to that in emissions of fossil diesel. Total biodiesel hydrocarbon emissions are 93% lower than fossil fuels [18–20].

Growing of biodiesel feedstock resources relies heavily on temperature, local soil conditions and availability; therefore, different regions are targeting different types of biodiesel feedstock. The extensive use of soybeans for food in the United States has led to the rise of soybean biodiesel there. Rapeseeds are Europe's most common feedstock for biodiesel production. The jatropha tree is used in the production of biodiesel in India and South East Asia. Palm oil is used as a major source of biodiesel in Malaysia and Indonesia. However, current biodiesel industries mostly depend on feedstocks made from food "feedstuffs", and these are known as first-generation biodiesel [21]. Although the available biodiesel spectrum shows the versatility and popularity of the biodiesel industry, this capability has not been fully adopted by first-generation biodiesel systems due to some social and environmental concerns. The main disadvantage of the first-generation biofuel is that it is made from edible oils, which has the effect of increasing food prices and also creates undue pressure on land use for food production. This issue is widely referred to as the "Food vs. Fuel" debate. Supply and demand determine that increasing production of biodiesel from food crops would increase the costs of food, a problem already faced by countries such as Malaysia. This topic was discussed globally as a result of the global food price crisis of 2007–2008 [22]. There are several other reasons for this problem and there is still much speculation around the increased use of biodiesel, food shortages and resulting price spikes. The proven advantages of biofuel and its ability to minimise reliance on fossil fuels has increased its demand; however, this should not lead to famine. Despite this, it is considered unlikely that this first-generation form of biodiesel will sustainably achieve its potential to contribute to socio-economic development. As a result, alternative feedstocks need to be explored to address the major supply limitations of first-generation biodiesels. Second-generation biodiesels are coming into focus in order to address this issue. These feedstocks are typically not edible, comprising non-food crops, forest residues and other biomass sources. Consequently, oil companies, governments and non-governmental organisations are beginning to invest more research funds in the development of second-generation biodiesels [23,24].

In a recent report, Anwar et. al., [25] carried out a detailed screening on different types of second-generation biodiesel feedstocks in relation to their compositional and

physicochemical characteristics. Rapeseed, beauty leaf, papaya, apricot, jatropha and waste cooking oil were the feedstocks examined in their study. Twelve physiochemical qualities were selected as parameters for the rating of biodiesel. This investigation found that apricot kernel oil was the best choice for the production of second-generation biodiesel among the examined feedstocks, followed by papaya oil. Apricot (*Prunus armeniaca*), belonging to the Rosaceae family, is widely grown around Australia, particularly in South Australia and Victoria. The fruits of apricot trees are also called stone fruits. From October to April, Australia grows approximately 100,000 tonnes of stone fruits per year. The fruits develop from a green fruit bud and mature to orange- and purple-coloured fruits with soft flesh covering a hard kernel. The fruits are usually round with a diameter of 15–25 mm; the orange flesh is separated in processing (tinned apricots), while the hard seed kernels are generally discarded during fruit processing due to the presence of hydro-cyanic acid [26]. However, this stone fruit kernel contains over 50% non-edible bio-oil that can be processed for biodiesel production [27]. Hence, stone fruit oil (SFO) has gained a large amount of research interest and a number of studies have therefore attempted to investigate the feasibility of inedible SFO for second-generation biodiesel. Wang and Yu [28] analysed the potential of SFO biodiesel and concluded that it provides a low-cost, high-oil and low-acid feedstock option for biodiesel production. Anwar et al. [29] studied the physicochemical properties of SFO biodiesel and found that it had high quality, comparable to that of commercially available biodiesel and concluded that SFO biodiesel satisfies both the ASTM D6751 and EN14214 standards in all terms of quality parameters. Singh Gurau et al. [30] studied the storage and oxidation stability of SFO biodiesel. They reported that SFO biodiesel is able to meet the requirements of ASTM D6751, IS15607 and EN14214 biodiesel specifications without the addition of an antioxidant, even after six months of storage in dark and sunlight conditions.

These results show that SFO has significant potential to become a low-cost feedstock for second-generation biodiesel production, and thus help to overcome the potential socio-economic challenges mentioned above. However, in order to establish a new feedstock for biodiesel production and also to start production at an industrial scale, it is necessary to confirm that this biodiesel can be used in diesel engines without any requirement for engine modifications.

Scientists have worked tirelessly in recent years to enhance engine performance and combustion efficiency, and to minimise exhaust gas emissions by investigating biodiesel–diesel blends of non-edible SFO. However, apricot-based SFO biodiesel has been comparatively less explored. An attempt was made by Gumus and Kasifoglu [31] when investigating engine performance and exhaust emissions using SFO biodiesel as fuel. SFO from Turkey was used as the feedstock for biodiesel production. A single cylinder diesel engine operated successfully using the SFO biodiesel without any modifications to the original diesel engine. This study found a better engine performance and lower exhaust emissions with SFO biodiesel compared to conventional diesel. However, this investigation was limited in presenting the experimental results from a single-cylinder small engine (0.395 dm³) and did not measure the particulate matter (PM) emissions, which are a critical concern in modern automobile engines [18]. Hazar et al. [32] conducted experiments on a three-cylinder 1.4 dm³ direct injection diesel engine with SFO biodiesel as fuel and showed that this biodiesel is also capable of being used in place of fossil diesel. This study also used SFO from Turkey for biodiesel production and did not record any experimental emission results for the PM count. In a recent study, Karishma et al. [33] carried out an investigation of different proportions of SFO biodiesel–diesel blends in a single-cylinder diesel engine. Their target was to find the best blend proportion that can partially replace the diesel fuel in a CI engine. Data from the investigations of several engine performance and emissions characteristics were taken into consideration to reach a conclusion. Finally, they found that 20% SFO biodiesel with 80% diesel was the combination that provided the best engine performance and emissions. However, investigation of the PM was also absent in their study. In order to fully understand the combustion characteristics of SFO

biodiesel, it is necessary to run a full-sized, automobile diesel engine on SFO biodiesel as part of the investigation of stringent performance and emission indicators. The information provided in the current literature is limited in this regard, and this may be a factor that has contributed to the lack of apricot-based SFO biodiesel production being established on a commercial scale. Therefore, this study aimed to fill the knowledge gap by providing an in-depth examination of SFO biodiesel in a diesel engine. Comprehensive thermodynamic and emission analyses on SFO biodiesel combustion were performed on important parameters including particulate matter emissions. This study is also a first in investigating apricot-based SFO biodiesel having an Australian origin. The results presented herein are therefore expected to advance the development of the regional energy sector through the creation of new scientific information based on low-cost SFO with significant potential as a sustainable second-generation biodiesel feedstock.

2. Materials and Methods

2.1. Production of SFO Biodiesel and Its Blends

The stone fruits were collected from the southern part of Australia and the fleshy sections were removed by hand. The seeds were separated and soaked in water for about half an hour in order to effectively remove the hard shells from the kernels. The kernels were then gathered and dried under sunlight for about 12 days to reduce the moisture content. Then, all the kernels were ground using a shredder to produce a particle size of <1 mm. A Soxhlet apparatus was used to extract oil from these ground kernels. The apparatus was operated at 60 °C and petroleum ether was used as solvent. The process was continued for 6–8 h until the extraction was completed. Then, the extracted oil was placed in a rotary evaporator to evaporate the petroleum ether. To remove any remaining solvent, an oven was utilised to heat the oil at 60 °C for about 60 min. Whatman 541 filter paper was also used to filter the oil. After filtering, the SFO was sealed in a container. The obtained SFO was then converted to biodiesel through the transesterification process using a 1 L three-neck laboratory reactor. Two chemicals, namely, methanol (MeOH, purity 99.9%) and potassium hydroxide (KOH pellets, purity 99%), were used in this conversion process. A mixture was prepared by dissolving KOH in MeOH. This mixture was added to the obtained SFO. The solution was prepared in a MeOH-to-SFO molar ratio of 6:1 and KOH catalyst concentration of 0.5 weight % (wt%). Then, this solution was poured into the reactor. The reactor was operated at 55 °C for about 40 min. To separate biodiesel from glycerol, the solution was collected in a separate funnel and cooled to room temperature. The thicker layer of glycerol that had collected at the bottom of the funnel was then separated. The produced biodiesel was washed with warm distilled water and reheated to 110 °C for 15 min to remove any water residue. The final conversion yield of biodiesel was 95.8%. Before being stored for characterisation, it was filtered through Whatman® qualitative Grade 1 paper. Figure 1 illustrates the SFO biodiesel production process.

The SFO biodiesel and its binary blends with diesel were made in accordance with the experimental design. The binary blends of SFO5, SFO10 and SFO20 were made by combining 5%, 10% and 20% vol. of SFO biodiesel with 95%, 90% and 80% vol. of diesel, respectively. Each binary blend was agitated for 60 min at 600 rpm using a magnetic stirrer. For each blend, a homogeneous mixture was observed, ensuring that no phase shift occurred for any binary blends.

The physicochemical properties of the obtained SFO biodiesel and its blends with diesel were determined by appropriate American standard of testing materials (ASTM) standards. Table 1 lists the measured properties along with respective ASTM standards and measuring tools.

In addition, a gas chromatograph (GC), model Thermo Scientific Trace 1310GC was used for fatty acid composition analysis and a Spectrum 100 FTIR spectrometer was used to determine Fourier transform infrared (FTIR) spectroscopy.



Figure 1. SFO biodiesel production process.

Table 1. Physicochemical properties, ASTM standards and measuring tools.

Properties	ASTM Standard	Measuring Tool
Calorific value	D240	6100EF semi-auto bomb calorimeter
Kinematic viscosity	D445	NVB classic
Density	D1298	DM40 LiquiPhysics™
Acid value	D664	Automation titration Rondo20
Flash point	D93	NPM 440 Pensky-Martens
Oxidation stability	D2274	873 Rancimat

2.2. Engine Setup and Experimental Procedure

A four-stroke, four-cylinder and naturally aspirated diesel engine (Kubota V3300, Kubota Australia, Osaka, Japan) was used in this study. Table 2 presents the details of the tested diesel engine specifications.

Table 2. Test engine specifications.

Items	Specifications
Model	Kubota V3300
Type	Vertical, 4 cycle liquid cooled diesel
No. of cylinders	4
Total displacement (m ³)	3318
Bore × Stroke (mm)	98 × 110
Combustion type	Spherical type [E-TVCS (Three vortex combustion system)]
Intake system	Naturally aspirated
Rated power output (kW.rpm ⁻¹)	53.90/2600
Rated torque (Nm.rpm ⁻¹)	230/1400
Compression ratio	22.60:1
Fuel injection timing	16° before top dead centre (TDC)
Injection pressure (MPa)	13.73
Emissions certification	Tier 2

The V3300 engine was coupled with an eddy current dynamometer manufactured by Dyno Dynamics (Melbourne, Australia). A TFX control system was used for data

acquisition. A CODA 5 gas analyser and a MAHA MPM-4M particulate matter meter were used for measuring exhaust gas emissions. The combustion characteristics were monitored using a piezoelectric pressure transducer and crank angle encoder. Figure 2 shows the schematic diagram of the experimental setup used in the present study.

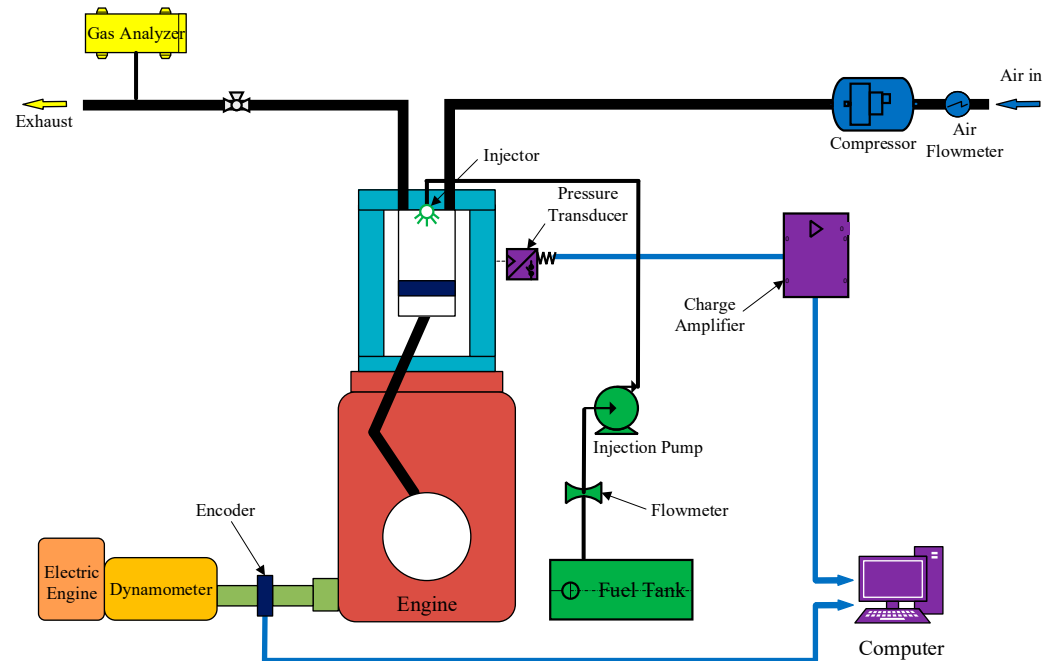


Figure 2. Schematic diagram of the experimental setup used in the present study.

Three binary SFO fuel samples along with reference diesel were tested in this engine. The tests were performed at 100% load and different engine speeds ranging from 1200 to 2400 rpm, at a 200 rpm interval. Each data collection was replicated three times and the average data were taken to prevent potential errors. Shortly after each experiment was completed, the engine was rinsed with pure diesel.

2.3. Error and Uncertainty

Errors or uncertainties in measurements may occur due to many factors related to instrument parts, calibration, observation or experimental condition, and procedure. To ensure the accuracy of the measurements, it is critical to analyse the uncertainties inherent in the measured values. In this study, the total uncertainty was calculated using Holman's technique [34], which was based on the method of propagating errors. Table 3 lists the errors and uncertainties associated with the instruments utilised in this study.

Table 3. Errors and uncertainties in the measurements created by different instruments.

Measuring Parameter	Range	Accuracy
Engine load	0–15 kg	±0.01 kg
Engine speed	0 rpm to 3000 rpm	±5 rpm
Crank angle	0–360°	±1°
Temperature	1–2000 °C	±1 °C
Pressure	0.5–100 bar	±0.01 bar
Air flow rate	16.00–32.00 kg·hr ⁻¹	±0.01 kg·hr ⁻¹
Fuel flow rate	0.1–1.5 kg·hr ⁻¹	±0.01 kg·hr ⁻¹
NO _x	0–5000 ppm	±1.0 ppm
HC	0–30000 ppm	±1.0 ppm
CO	0–15%	±0.02%
CO ₂	0–20%	±0.30%
PM	<100 nm to >10 µm	±0.10 nm

Table 3. Cont.

Calculated Parameter	Range	Uncertainty
Brake power (BP)	-	0.90%
Torque	-	0.90%
Brake specific fuel consumption (BSFC)	-	1.15%
Brake thermal efficiency (BTE)	-	1.15%

3. Results and Discussion

3.1. Characterisation Properties and Fatty Acid Composition of SFO Biodiesel and Its Blends

SFO biodiesel blend properties are shown in Table 4. Normally, biodiesel has higher density and viscosity than diesel; the results of this study were in agreement with this, as the produced SFO biodiesel has 3.36% higher density and 31.8% higher viscosity compared with the reference diesel. Higher density can increase the energy concentration of fuel and causes higher viscosity, which leads to poor combustion, in addition to lower engine performance with excessive exhaust emissions [35]. Some research found that the higher viscosity of biodiesel can enhance the fuel spray penetration, resulting in improvement in the air–fuel mixture, which explains the recovery of brake power (BP) and torque in comparison with diesel [36–38]. Other contradictory findings also claimed that higher viscosity of fuel resulted in producing lower BP and decreased combustion efficiency due to poor fuel injection atomisation [39,40].

Table 4. Fuel properties of SFO biodiesel blends compared with international standards.

Fuels	Density (kg·m ⁻³)	Viscosity at 40 °C, mm ² ·s ⁻¹	Acid Value, mg KOH·g ⁻¹	Cetane Number (CN)	Calorific Value, MJ·Kg ⁻¹	Flash Point, °C	Iodine Value (IV) mgI ₂ ·100 g ⁻¹	Oxidation Stability (OS), h
SFO	855.0	4.26	0.25	50.45	39.64	105	104.70	7.15
SFO5	827.2	3.28	0.06	48.12	45.02	70.33	41.62	37.41
SFO10	829.9	3.33	0.07	48.25	44.73	72.15	44.94	35.82
SFO20	832.7	3.44	0.09	48.49	44.17	75.80	51.58	32.63
Ref. diesel	827.2	3.23	0.05	48.00	45.30	68.5	38.3	39.0
ASTM D6751	880.0	1.9–6.0	max. 0.5	min. 47	-	100–170	-	min. 3
EN14214	860~ or ~900	3.5–5.0	max. 0.5	min. 51	35	min. 101	max. 120	min. 6
AU Standard	860~ or ~890	3.5–5.0	max. 0.8	min. 51	-	min. 120	max. 120	min. 6

The acid value found for SFO biodiesel was 0.25 mg KOH·g⁻¹, which indicates the free fatty acid (FFA) contents. Both ASTM and EN standards have the highest limit of 0.5 mg KOH/g, whereas the Australian standard is for a maximum of 0.8 mg KOH·g⁻¹.

Higher acid values can cause corrosion of a diesel engine and its parts, and is detrimental to the longevity of the engine. The cetane number (CN) directly relates to ignition delay (ID), with higher CN ensuring shorter ID and enhanced combustion. The literature shows that biodiesels usually exhibit a higher CN compared to diesel fuel due to long-chain HC groups [35]. SFO biodiesel has a 5.1% higher CN than the reference diesel in this study. The calorific value of any fuel is the most influential parameter, as it denotes the releasing energy available for producing work. A lower BP was found due to lower calorific value for any biodiesel blends.

The calorific value of the produced SFO biodiesel is 12.5% lower than that of diesel. Furthermore, the flash point of a fuel plays an important role in transportation, storage and handling. A higher flash point ensures the greater safety of the fuel. The SFO biodiesel has a 53.3% higher flash point, which indicates the methanol content and viscosity are related to unreacted triglycerides. The iodine value found for SFO biodiesel was 104.70 mgI₂/100 g, which sits within the limits of the EN and Australian standards. SFO biodiesel has an iodine value that is more than 2.7 times higher; this ensures a better fuel quality due to a more saturated double bond than that of diesel. The oxidation stability (OS) of SFO was recorded at 7.15 h, which is higher than the minimum set values from ASTM, EN and AU standards. The higher OS ensures a better quality of the fuel.

Figure 3 shows the chromatogram of the SFO and its formation of methyl esters, i.e., biodiesel. The presence of derivatives of C 16:0 (palmitic acid), C 18:0 (stearic acid), C 18:1 (oleic acid), C 18:2 (linoleic acid), C 18:3 (linolenic acid) and C 22:1 (behenic acid) is evident in the GC profile. Fatty acid composition (FAC) depends on several factors such as feedstock quality, its growing conditions, climatic conditions and location. FAC determines the quality of the oil and its properties.

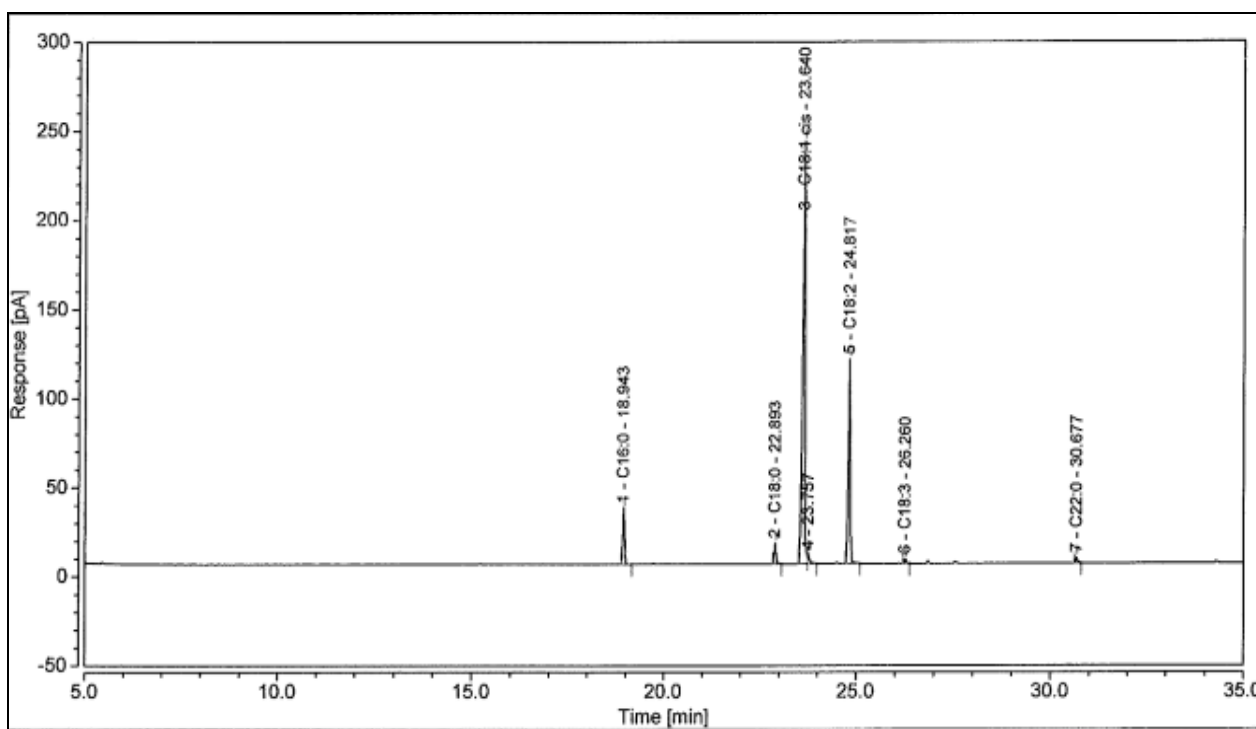


Figure 3. GC profile of SFO biodiesel.

The FAC of SFO biodiesel or methyl ester profile is presented in Table 5. SFO biodiesels are mainly comprised of oleic acid (63.8%) and linoleic acid (25.3%). The saturated fatty acid content was found to be 9.02% and total unsaturated (mono- and poly-) fatty acid content was found to be 89.7%. The degree of unsaturation was recorded at 115.5 °C, and this has a substantial effect on combustion profiles and exhaust gases. A higher saturation relates to the higher CN of the biodiesel. The unsaturated biodiesels produce higher NO_x and lower HC emissions than those of saturated biodiesels [41,42].

Table 5. The fatty acid composition of SFO biodiesel.

Fatty Acids	Formula	Molecular Weight	Structure	wt%
Palmitic	C ₁₆ H ₃₂ O ₂	256	16:0	5.85
Stearic	C ₁₈ H ₃₆ O ₂	284	18:0	2.51
Oleic	C ₁₈ H ₃₄ O ₂	282	18:1	63.8
Linoleic	C ₁₈ H ₃₂ O ₂	280	18:2	25.3
Linolenic	C ₁₈ H ₃₀ O ₂	278	18:3	0.51
Behenic	C ₂₂ H ₄₄ O ₂	340	22:0	0.66
Others				1.29
Total Saturated Fatty Acids (SFA)				9.02
Total Monounsaturated Fatty Acids (MUFA)				63.84
Total Polyunsaturated Fatty Acids (PUFA)				25.85
The Degree of Unsaturation (DU)				115.5
Long Chain Saturated Factor (LCSF)				2.83

The FTIR spectrum of SFO biodiesel is presented in Figure 4. The asymmetric stretching of $-\text{CH}_3$ was found to be present at 1435.8 cm^{-1} . The CH_3 asymmetric stretching vibration was observed in the $2800\text{--}3000\text{ cm}^{-1}$ region. The stretching of the carbonyl group ($-\text{C}=\text{O}$) was at 1742 cm^{-1} in the region of $1800\text{--}1700\text{ cm}^{-1}$, which confirms with the ester formation. Details of the FTIR spectrum results can be found in Anwar et al. [41]. FTIR results confirm the conversion of triglycerides to methyl esters.

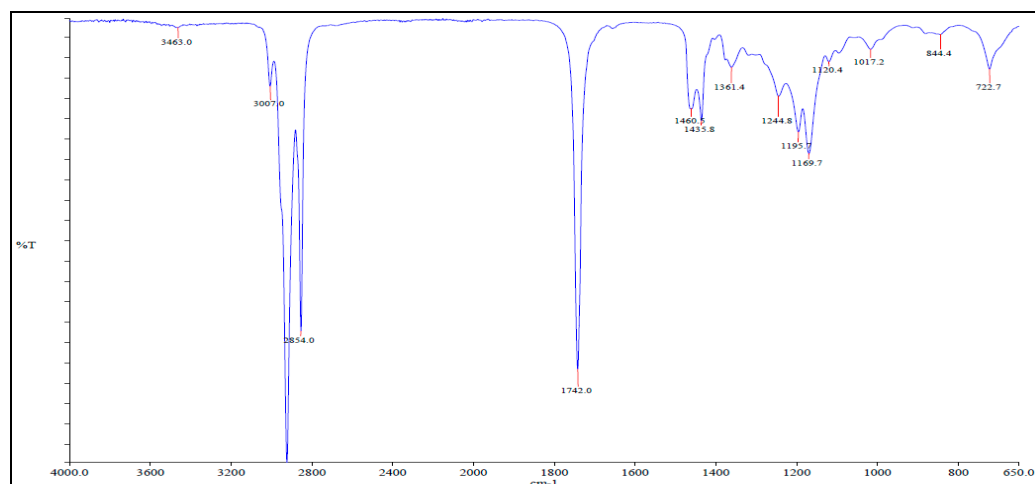


Figure 4. Fourier transform infrared (FTIR) spectrum of SFO biodiesel.

3.2. Engine Performance

Figure 5i illustrates the variation of BP with engine speeds for all four blends at 100% engine load level. With the rise in engine speeds, the BP gradually improved across all fuel blending. The lower the amount of biodiesel present in the blend, the higher the BP value [39,43,44]. The diesel showed the highest BP value under all specified engine speeds, followed by SFO5, SFO10 and SFO20. The average BP values for SFO5, SFO10, SFO20 and diesel were 38.34, 37.9, 37.42 and 39.25 kW, respectively. The average BP reduction for SFO5, SFO10 and SFO20 was 2.3%, 3.4% and 4.67%, respectively, compared with that of diesel, due to higher density/viscosity, and lower calorific values of biodiesel; this is evidenced by other researchers [45–48]. Higher viscosity reduced the combustion efficiency due to the poor fuel injection atomisation, resulting in a lower BP value [39,40].

Figure 5ii represents engine torque vs. speed at 100% loading condition. It was observed that torque increased with engine speed up to 1400 rpm and decreased gradually with increases to 2400 rpm for all four blends due to friction loss and reduction in volumetric efficiency [45,49,50]. Torque decreased when the amount of biodiesel in the blends was increased [51]. In contrast, diesel showed the highest torque at all engine speeds as compared with SFO5, SFO10 and SFO20. The average torque recorded values were 205.42, 203.16, 200.5 and 207.86 Nm for SFO5, SFO10, SFO20 and diesel, respectively. The average decreases in torque values for SFO5, SFO10 and SFO20 were 1.17%, 2.26% and 3.54%, respectively. Researchers have found that, due to higher calorific values, lower densities and viscosities of diesel, the engine torque was higher [47,49,50].

Figure 5iii indicates that the brake specific fuel consumption (BSFC) increases with engine speeds. Ong et al. [52] reported that the degradation in combustion occurs at higher BSFCs and friction heat losses arise at higher speed. Other researchers have suggested that the injection system, density, viscosity and calorific value have significant impacts on BSFC [53–55]. A higher BSFC was observed due to lower calorific value of biodiesel, which required more fuel to achieve the same power as diesel. Yet again, diesel showed the lowest BSFC as compared to SFO5, SFO10 and SFO20 for all engine speeds. The average BSFC values for SFO5, SFO10, SFO20 and diesel were 268.67, 276.12, 296.05, and 256.54 g.kWh^{-1} , respectively. The average increases in BSFC for SFO5, SFO10 and SFO20 were 4.73%, 7.63% and 15.4%, respectively, in comparison with diesel.

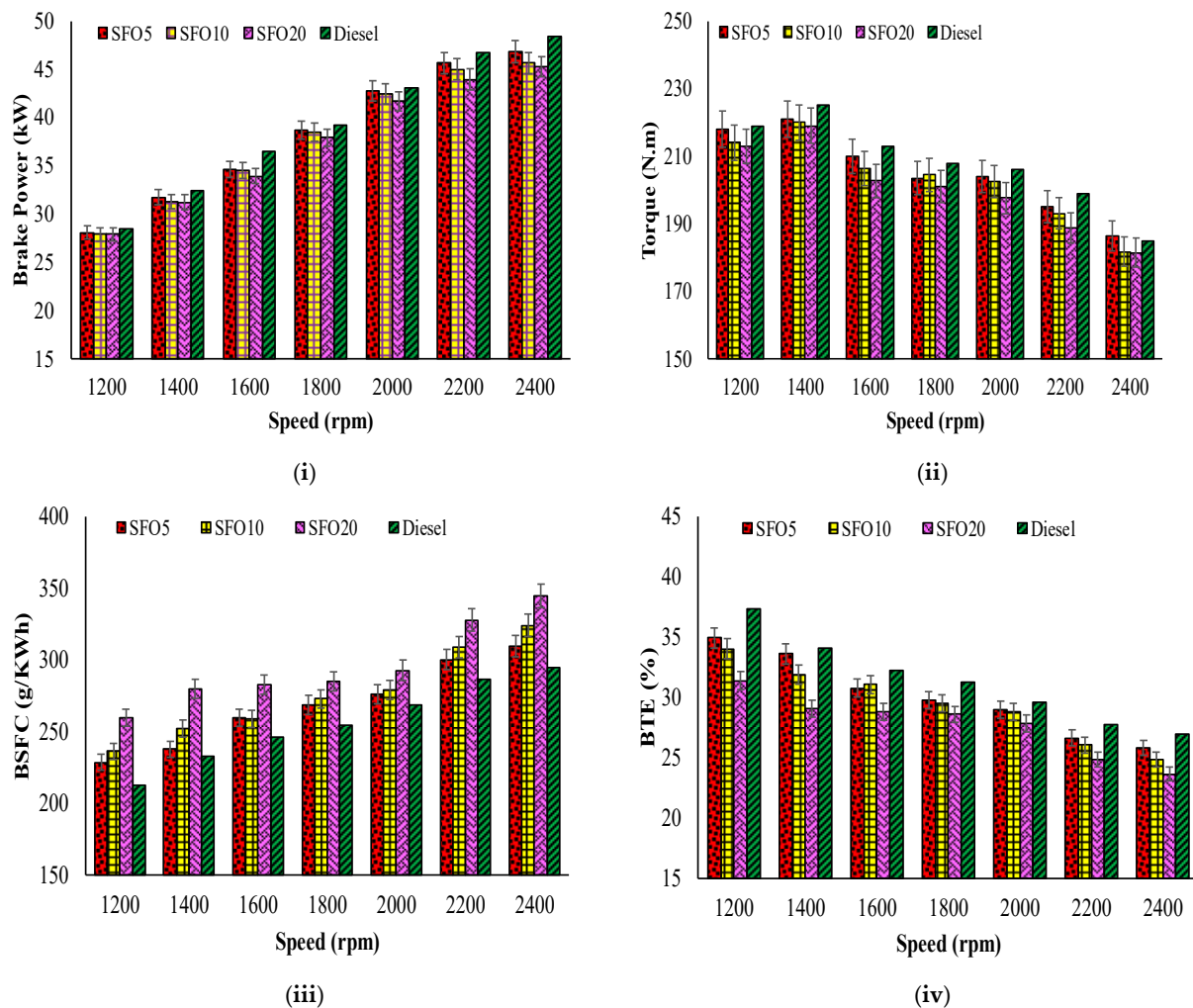


Figure 5. Variation in engine performance with engine speeds.

The variations in brake thermal efficiency (BTE) vs. speed for all four blends at 100% load condition are seen in Figure 5iv. This shows that BTE decreased when engine speed increased. Researchers have indicated that, at higher engine speeds, BTE decreases due to a lack of sufficient air resulting in incomplete combustion [56,57]. Again, higher BTE is observed due to higher calorific value, and lower density and viscosity. A higher BTE is found at a lower biodiesel content due to the higher calorific value and lower fuel consumption. Again, some studies have found that, due to lower viscosity and reduced stability, improved air–fuel mixtures are ensured, resulting in better combustion [52,58]. As predicted, diesel showed the highest BTE compared to SFO5, SFO10 and SFO20 at all engine speeds. The average BTE values for SFO5, SFO10, SFO20 and diesel were 30.08%, 29.56%, 27.75% and 31.33%, respectively. The average BTE decreases for SFO5, SFO10 and SFO20 relative to diesel were 3.97%, 5.98% and 11.41%, respectively.

3.3. Emission Characteristics

Figure 6i indicates differences in exhaust gas temperature (EGT) vs. engine speed for the SFO biodiesel and diesel blends. The trend of the EGT profile increases with speed due to the higher fuel quantity required per unit of time to achieve higher heat energy in the combustion chamber, which was observed by Ong et al. [59]. Conversely, the higher the amount of biodiesel in the mix, the greater the EGT. Once again, pure biodiesel (100%) has lower heating values, and higher density and viscosity, resulting in a reduction in atomisation and incomplete combustion, leading to higher EGTs [52,60]. Ong et al. [59]

stated that diesel has a lower EGT in comparison with all the tested fuels due to higher heating value and shorter combustion period. The average EGTs were reported as 577.54, 592.93, 607.86 and 572.60 °C for SFO5, SFO10, SFO20 and diesel, respectively. The average increases in EGT for SFO5, SFO10 and SFO20 were 0.87%, 3.56% and 6.16%, respectively, relative to diesel.

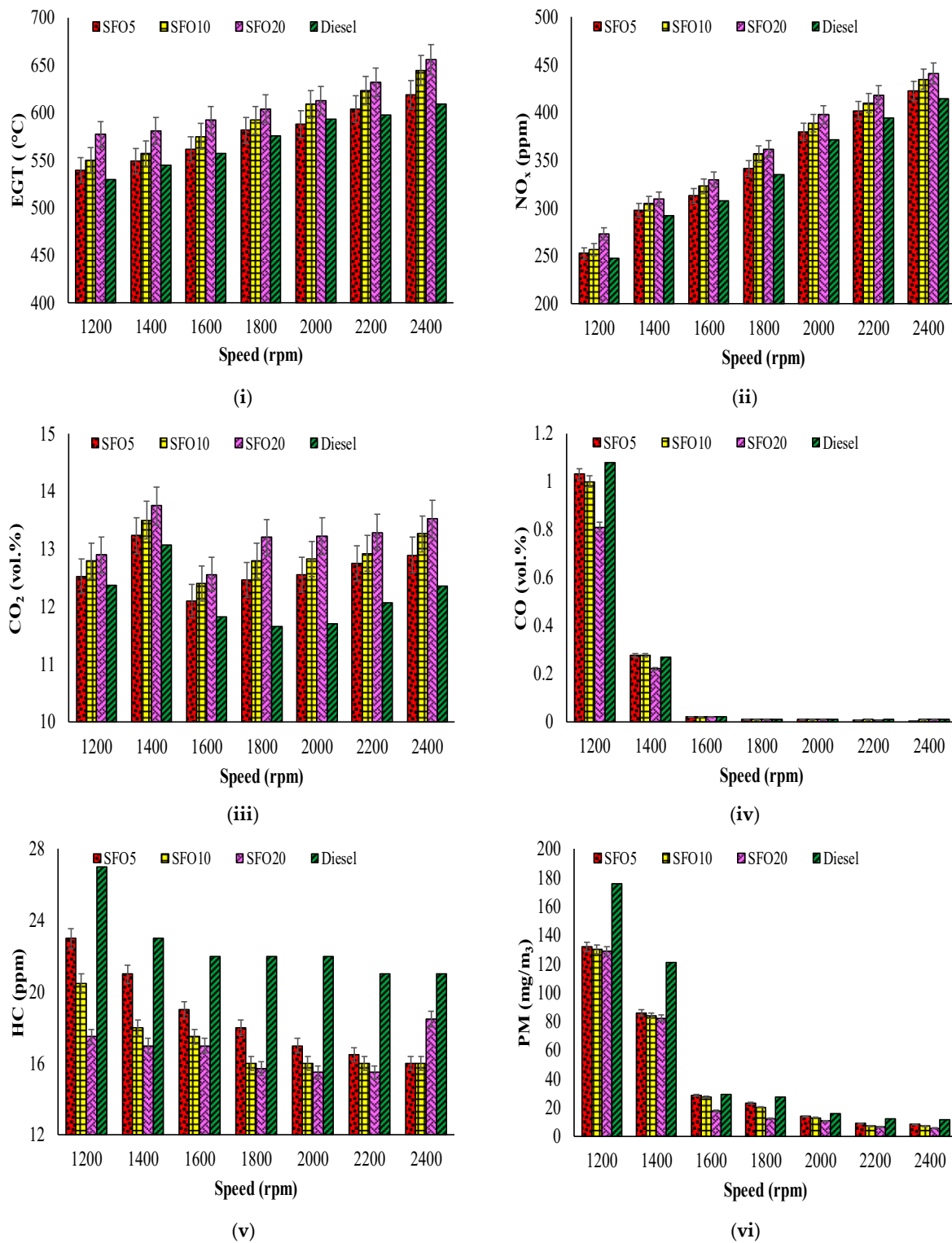


Figure 6. Variation in engine emissions with engine speeds.

NO_x emissions are produced due to peak in-cylinder temperature and oxygen concentration. Generally, biodiesels have higher oxygen content, which is a cause of higher NO_x emissions. The NO_x increases with engine speeds due to high in-cylinder turbulence, higher combustion temperatures and stoichiometry of the mixture; this increase results in a homogenous air–fuel mixture [55,61]. At 100% engine load, the air–fuel ratio improved, which culminated in higher gas temperatures in the chamber and the production of more NO_x emissions [62,63]. The changes in NO_x emissions with speed for the SFO blends with diesel at 100% engine load are seen in Figure 6ii. Higher biodiesel content in blends results in higher NO_x emissions due to higher viscosity, density and bulk modulus, which lead to early fuel injection. This causes early combustion and results in increased NO_x output [64]. Other researchers [31,62] also concluded that higher contents of biodiesel in blends cause increased NO_x emissions. However, the higher cetane content of low biodiesel blends may have caused a short ignition delay (ID), which induced the combustion temperature and pressure, hence resulting in less NO_x output [65]. The average concentrations of NO_x emitted by SFO5, SFO10, SFO20 and diesel were respectively 344.43, 353.72, 361.72 and 337.86 ppm. The average NO_x pollution increases for SFO5, SFO10 and SFO20 relative to diesel were 1.95%, 4.69% and 7.06%.

CO₂ emissions are a significant parameter indicating a fuel's combustion efficiency, as higher CO₂ corresponds to better combustion [36]. Figure 6iii shows the CO₂ emissions of the tested fuels across all engine speeds. At a maximum rated torque of 1400 rpm, the highest CO₂ emissions for all blends were recorded. The higher the amount of biodiesel in the blend, the higher the CO₂ emissions, which contributed to the higher level of oxygen and CN in the biodiesel mixtures. Other researchers also reported higher CO₂ emissions due to more efficient combustion [66,67]. The total CO₂ emissions of SFO5, SFO10, SFO20 and diesel were 12.64%, 12.93%, 13.21% and 12.15%, respectively. The average increases in CO₂ emissions for SFO5, SFO10 and SFO20 were 4.09%, 6.45% and 8.72%, respectively, relative to diesel.

The CO emissions relate specifically to fuel type, engine speed, air–fuel mix, injection pressure and timing [31,44]. Biodiesel blends typically have a higher O₂ content and CN, which allows combustion to be completed and results in lower CO emissions compared to diesel [68–70]. Figure 6iv indicates the variation in CO emissions across the range of engine speeds. With the rise in engine speeds, the CO emissions drop significantly, with the maximum emissions recorded at 1200 rpm; these are significantly reduced by 1400 rpm, then become insignificant at higher engine speeds. This is attributed to better mixtures of air–fuel happening at the higher engine speeds [68,71,72]. The average CO emissions from SFO5, SFO10, SFO20 and diesel were 0.194%, 0.191%, 0.155% and 0.202%, respectively. The average decreases in CO emissions for SFO5, SFO10 and SFO20 were 3.87%, 5.25% and 23.05%, respectively, relative to diesel.

The unburned hydrocarbon (HC) emissions primarily arise due to incomplete combustion as flame quenching occurs on the wall of the cylinder and in-cylinder crevices. For all four blends, the difference in HC emissions with engine speed are seen in Figure 6v at full (100%) loading operation. The HC emissions decrease as the engine speed increases. Koçak et al. [73] stated that higher fuel density and viscosity have a critical impact on fuel atomisation and ignition in the combustion chamber at lower engine speeds, resulting in higher HC emissions levels. Other researchers reported that an increase in chain length or biodiesel saturation level can lead to a greater reduction in HC emissions [74]. Lower HC emissions likely occur because of the higher oxygen content in biodiesel [31,43]. A higher cetane number of any biodiesel can reduce the burning delay, also resulting in lower HC emissions [75,76]. The average emissions of HC produced by SFO5, SFO10, SFO20 and diesel were respectively 18.64, 17.14, 16.67 and 22.57 ppm. The average decreases in HC emissions for SFO5, SFO10 and SFO20 relative to diesel were 17.4%, 24.06% and 26.14%, respectively.

In biodiesel blends, PM emissions are usually lower than in diesel due to lower volatility and higher oxygen content [77]. Figure 6vi demonstrates the variability in the PM

emissions over engine speeds for all four fuel blends at 100% engine load conditions. The PM emissions decrease when the engine speed rises [71,78]. Lin et al. [79] stated that the higher CN in biodiesel blends may cause a shorter ignition delay and longer combustion, resulting in lower PM emissions. The average concentrations of PM produced by SFO5, SFO10, SFO20 and diesel were, respectively, 43, 41.33, 37.86 and 56.18 $\text{mg}\cdot\text{m}^{-3}$. The average decreases in PM emissions for SFO5, SFO10 and SFO20 were 23.43%, 26.43% and 32.62%, respectively, relative to diesel.

3.4. Combustion Behaviour

Figure 7i indicates variations in pressure inside the combustion chamber due to adjustments in the angle of the crankshaft at 100% engine load and at 1400 rpm (the rpm at which the engine generates the highest torque) and at maximum engine speed (2400 rpm). Figure 8i allows three torque ranges to be distinguished. At 1400 rpm, pure diesel generates the maximum pressure. Lowest pressure is created by SFO20, whereas SFO5 and SFO10 generate very similar pressures. Murillo et al. [80] found that, because diesel LHV is 13.5% higher than that of SFO20, SFO20 provided the lower in-cylinder pressure (CP) relative to pure diesel at maximum load. The literature shows that diesel blends with lower concentrations of biodiesel result in a slightly reduction in CP; this decrement was almost unnoticeable [36].

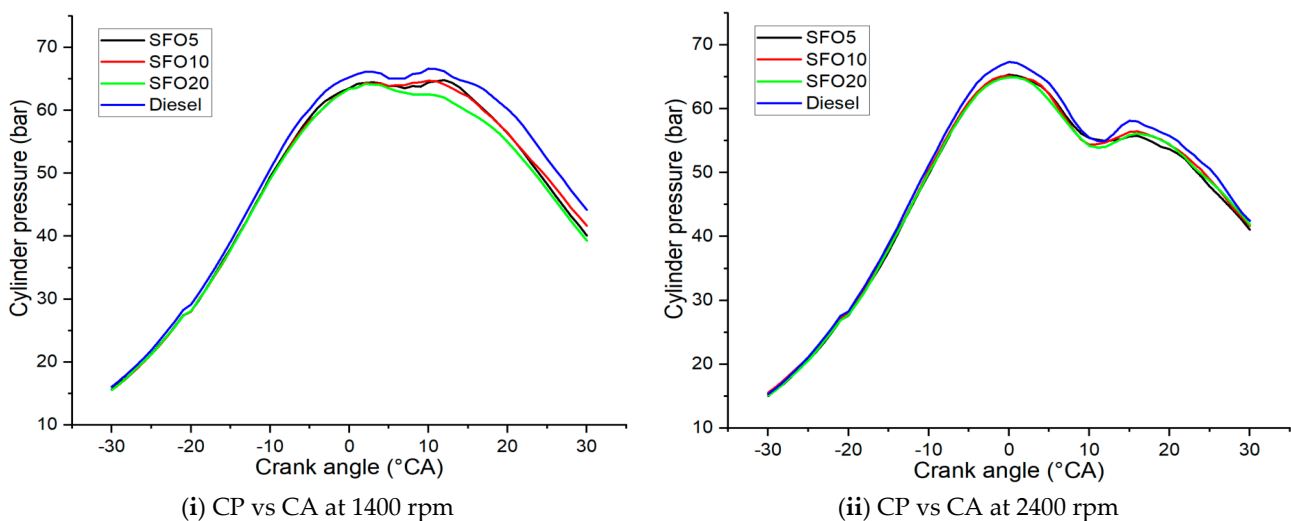


Figure 7. Variations in in-cylinder pressure with crank angle for SFO blends and diesel under 100% engine load at speeds of (i) 1400 rpm and (ii) 2400 rpm.

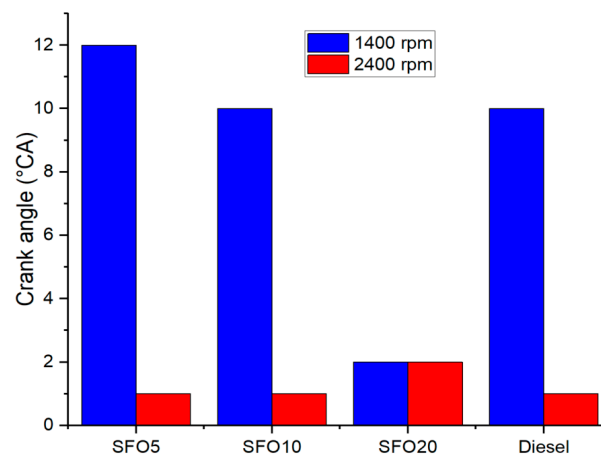


Figure 8. CA corresponding to the maximum in-cylinder pressure for the studied fuels at speeds of 1400 and 2400 rpm.

Figure 7ii shows that two pressure ranges could be distinguished at 2400 rpm. Pure diesel can be seen to produce more pressure inside the cylinder than all of the biodiesel blends, and this is due to diesel having a higher LHV compared to the biodiesel blends. All three biodiesel blends, however, had the same average pressure inside the cylinder and the difference between them was not great. This action may be related to the fact that, due to the high viscosity and high density of biodiesel and the lack of appropriate injection pressure for fuel atomisation at 2400 rpm, combustion is incomplete and the CP does not change with the change in the percentage of biodiesel in the blends [67].

Comparing the two sets of statistics, it can be observed that the height of the in-cylinder pressure at 1400 rpm occurs at the mixing-regulated combustion time, which is about 67 bar, whereas this value is about 55 bar at 2400 rpm. Since combustion in the mixing-controlled period is even more critical than the pre-mixed period, this results in increased torque [81].

Figure 8 shows the corresponding crank angle to the maximum pressure (CAMCP). As can be seen, with the increase from 1400 to 2400 rpm, the maximum pressure occurred at angles closer to the top dead centre (TDC). An increase in engine speed improves injection, which reduces combustion duration (CD), and the crank angle (CA) of maximum cylinder pressure (CP) will be closer to TDC [82]. Moreover, there is a significant difference between SFO20 and the other fuels, with the CA for SFO20 being sharply reduced. For SFO20 fuel, the CA of the peak CP is closer to TDC, and this is attributed to the fact that the positive effects of SFO20 properties, such as the high oxygen content and the low flash point, result in early combustion [83].

Figure 9 shows the changes in the HRR for different fuels at 100% engine load, and at 1400 and 2400 rpm. Figure 9i,ii show that the SFO20 blend has the highest amount of HRR. At 1400 and 2400 rpm, the highest peak HRR for SFO20 was measured as roughly $200 \text{ J} \cdot \text{°CA}^{-1}$ at 16° after top dead centre (ATDC) and as $250 \text{ (J} \cdot \text{°CA}^{-1})$ at 14° ATDC. A complete burning of this air–fuel mixture in-chamber may lead to an increase in the heat release rate (HRR) due to additional oxygen molecules in the biodiesels [84,85]. The internal air velocity of the engine combustion chamber increases if the engine speed increases. Higher engine speeds result in faster in-cylinder charge motions, superior fuel–air mixing, more complete combustion and higher HRR [86].

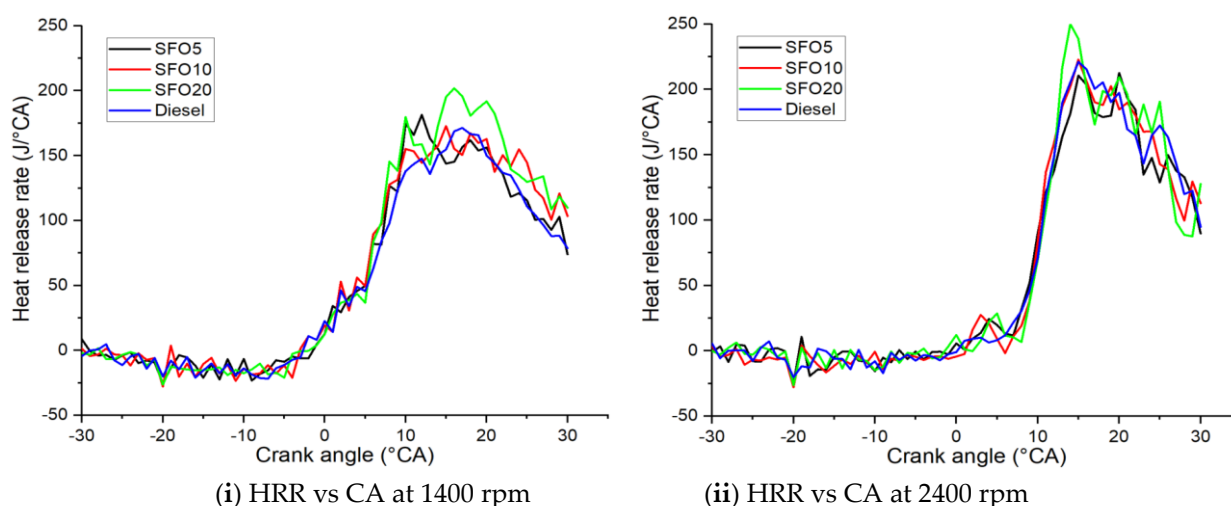


Figure 9. The variations in HRR for SFO blends and diesel under 100% engine load at speeds of (i) 1400 rpm and (ii) 2400 rpm.

Figure 10 shows the changes in temperature inside the combustion chamber in terms of degrees Celsius and the changes in the crankshaft circulation. Figure 10 reveals that the upward trend in temperature is slow up to about 8° CA , and then the slope increases so much that the temperature suddenly rises from about 800 to 1600° C over the rotation of 25° CA . As expected, the predicted values of the maximum temperature inside the combustion

chamber for the SFO20 mixture are the highest, which corresponds to the sudden increase in the measured NO_x produced by this fuel blend. In addition to the internal temperature of the combustion chamber, the production mechanism in the internal combustion engine also depends on the amount of oxygen. By increasing the concentration of biodiesel from 0% to 20% (Figure 11), the combustion chamber temperature increases and the amount of NO_x increases mutually; the presence of biodiesel oxygen is more effective and causes the decomposition of two-atom nitrogen and more production [87].

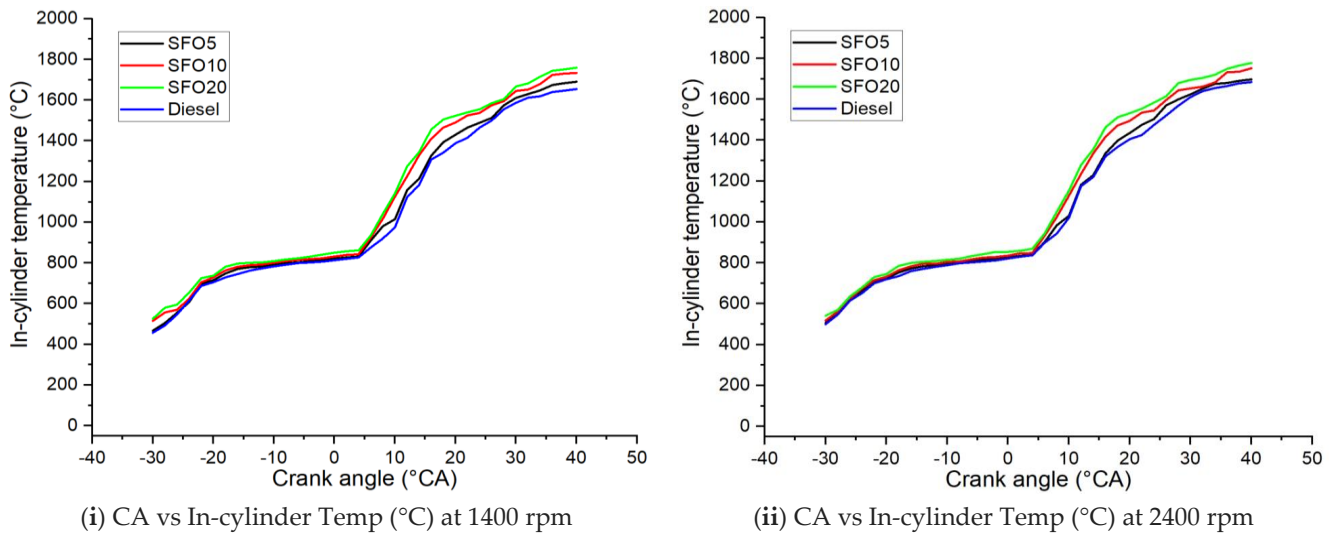


Figure 10. The variations in in-cylinder temperature for SFO blends and diesel under 100% engine load at speeds of (i) 1400 rpm and (ii) 2400 rpm.

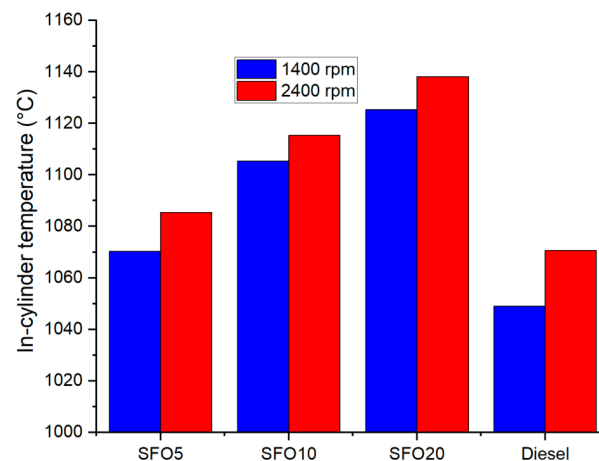


Figure 11. The average variation in the in-cylinder temperature for different fuels at 1400 and 2400 rpm.

The correlations between mass fraction burned (MFB) and CA at 1400 and 2400 rpm for the stoichiometric mixtures are shown in Figure 12i,ii. With an increase in the crank angle, at the start of combustion (SOC) process, there is a flame development duration where the MFB increases until reaching the maximum constant value of approximately one (≈ 1). This is put down to the fact that the flame propagation is enhanced with higher engine speed [88]. As evidence, the mass fraction burned at 2400 rpm reached the maximum of one (1) at 70 ATDC, which is much shorter than the 85 ATDC achieved at 1400 rpm due to the slower burning velocity. This discussion is supported by a close comparison between Figure 13i,ii. The total combustion duration, which is the sum of flame development duration (0–10% mass fraction burnt) and rapid burn duration (10–90% mass fraction

burnt) starts from -5° before top dead centre (BTDC) and progresses to 85° ATDC (90° CA) at 1400 rpm; however, at 2400 rpm; it begins at TDC and progresses to 75° after dead centre (ADC) (75° CA).

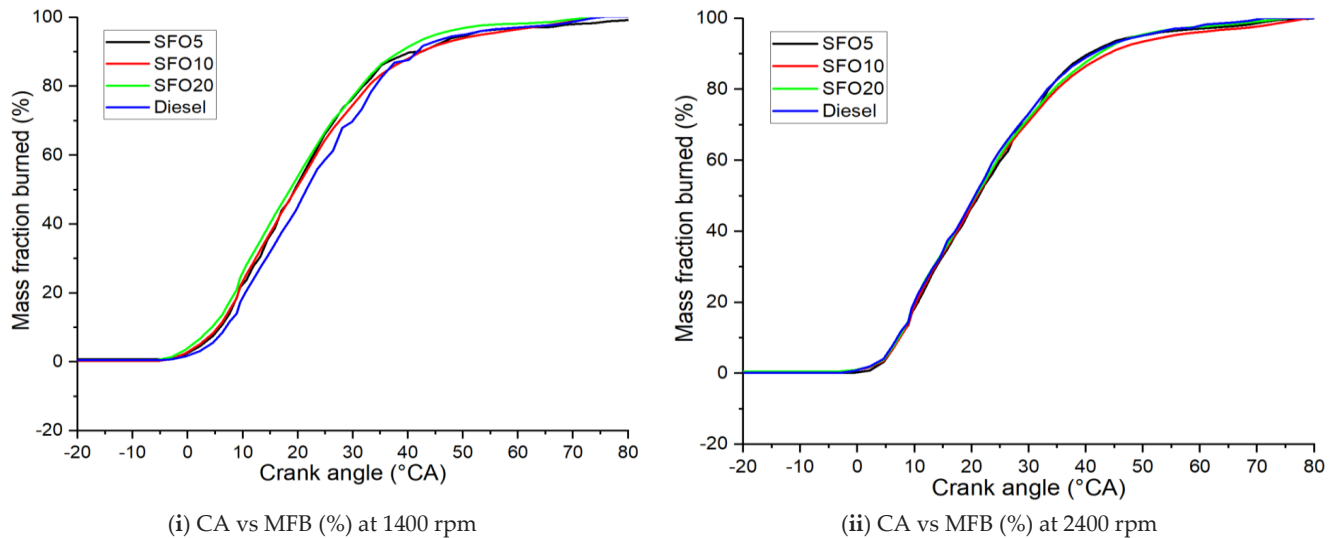


Figure 12. The variations in mass fraction burned (%) for SFO blends and diesel under 100% engine load at speeds of (i) 1400 rpm and (ii) 2400 rpm.

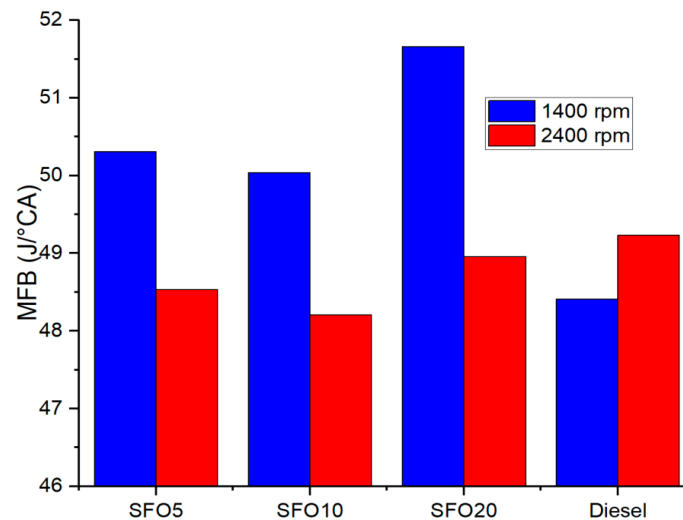


Figure 13. The average variation in the mass fraction burnt for different fuels at 1400 and 2400 rpm.

The average variations in the mass fraction burnt for different fuels are given in Figure 13. The differences in mass fraction burnt for 2400 rpm are closer to each other than for 1400 rpm, which means the higher speed resulted in the highest rate of burning and caused the highest efficiency rate of combustion [89]. The mass fraction burnt of biodiesels is increased with an increase in biodiesel percentage. The combustion is better sustained in the diffusive combustion phase due to the higher oxygen content of the higher biodiesel blends [82].

4. Conclusions

A fully instrumented four-stroke four-cylinder Kubota V3300 diesel engine was utilised in this study to investigate the potential of SFO biodiesel as an engine fuel. Three binary SFO biodiesel blends (5%, 10% and 20% *v/v* of biodiesel in diesel) and reference

diesel were tested at 100% engine load condition. Based on the findings obtained from this study, the following conclusions can be drawn:

- The analysis of the physicochemical properties of SFO biodiesel revealed that it fulfilled all international standards (ASTM D6751-2, EN 14214 and Australian biodiesel standard). The chromatogram of SFO biodiesel confirmed the formation of methyl esters. The fatty acid compositional analysis of SFO biodiesel indicates a high level (89.7%) of unsaturated fatty acids with high oleic acid content (63.8%).
- The average BP reductions for SFO5, SFO10 and SFO20 relative to diesel were 2.3%, 3.4% and 4.67%, respectively, which are attributed to higher biodiesel blends with lower calorific values, higher viscosities and higher densities. The average decreases in torque values for SFO5, SFO10 and SFO20 relative to diesel were 1.17%, 2.26% and 3.54%, respectively. The average increases in BSFC values for SFO5, SFO10 and SFO20 compared to diesel were 4.73%, 7.63% and 15.4%, respectively. Diesel had the highest BTE of all engine speeds followed by SFO5, SFO10 and SFO20.
- The average increases in EGT values for SFO5, SFO10 and SFO20 were 0.87%, 3.56% and 6.16%, respectively, relative to diesel. The NO_x and CO₂ emissions were increased, whereas the CO and HC emissions were decreased, with the increase in the biodiesel percentage in the fuel blends. Due to lower volatility and higher oxygen content, the PM emissions were also decreased and the average decreases were 23.43%, 26.43% and 32.62%, respectively, for SFO5, SFO10 and SFO20 relative to diesel.
- The SFO20 biodiesel blend had the highest cylinder pressure among the fuels tested. Combustion delay time for SFO20 fuel was less than that for other fuels, whereas diesel had the longest combustion delay. It was evident that, as the concentration of biodiesel increased, the duration of combustion also increased. The results revealed that SFO20 produced the highest in-cylinder temperature due to its highest HRR. These results also demonstrated that the highest MFB was related to SFO20.

Therefore, it can be said that SFO biodiesel is an excellent choice that has the potential to partially replace diesel fuel without any engine modifications. It can mitigate most of the environmental emissions and also utilise the waste seeds from the processing of the apricot fruit in the best possible way by turning fruit into an alternative energy source.

Author Contributions: Conceptualization, A.G.M.B.M.; Formal analysis, M.I.J., M.M.H. and R.K.; Investigation, D.S.; Writing—original draft, M.A.; Writing—review & editing, M.G.R., N.M.S.H. and R.H. All authors have read and agreed to the published version of the manuscript.

Funding: This research received no external funding.

Institutional Review Board Statement: No animal was involved in this study.

Informed Consent Statement: Informed consent was obtained from all subjects involved in the study from our department of the facility for the experimental activities.

Acknowledgments: The authors would like to acknowledge Tim McSweeney, Adjunct Research Fellow, Tertiary Education Division at Central Queensland University, Australia for his contribution in proof reading this article.

Conflicts of Interest: The authors declare no conflict of interest.

References

1. BP Energy Outlook 2040. Available online: <https://www.bp.com/content/dam/bp/business-sites/en/global/corporate/pdfs/energy-economics/energy-outlook/bp-energy-outlook-2019.pdf> (accessed on 1 May 2019).
2. Demirbas, A. Progress and recent trends in biofuels. *Prog. Energy Combust. Sci.* **2007**, *33*, 1–18. [[CrossRef](#)]
3. Zabeed, H.M.; Akter, S.; Yun, J.; Zhang, G.; Awad, F.N.; Qi, X.; Sahu, J.N. Recent advances in biological pretreatment of microalgae and lignocellulosic biomass for biofuel production. *Renew. Sustain. Energy Rev.* **2019**, *105*, 105–128. [[CrossRef](#)]
4. Abdullah, B.; Syed Muhammad, S.A.F.a.; Shokravi, Z.; Ismail, S.; Kassim, K.A.; Mahmood, A.N.; Aziz, M.M.A. Fourth generation biofuel: A review on risks and mitigation strategies. *Renew. Sustain. Energy Rev.* **2019**, *107*, 37–50. [[CrossRef](#)]
5. Jahirul, M.I.; Rasul, M.G.; Chowdhury, A.A.; Ashwath, N. Biofuels Production through Biomass Pyrolysis—A Technological Review. *Energies* **2012**, *5*, 4952–5001. [[CrossRef](#)]

6. Bhuiya, M.M.K.; Rasul, M.G.; Khan, M.M.K.; Ashwath, N.; Azad, A.K. Prospects of 2nd generation biodiesel as a sustainable fuel—Part: 1 selection of feedstocks, oil extraction techniques and conversion technologies. *Renew. Sustain. Energy Rev.* **2016**, *55*, 1109–1128. [[CrossRef](#)]
7. Anwar, M.; Rasul, M.G.; Ashwath, N. Production optimization and quality assessment of papaya (*Carica papaya*) biodiesel with response surface methodology. *Energy Convers. Manag.* **2018**, *156*, 103–112. [[CrossRef](#)]
8. Li, J.; Chen, X.; Yi, Z.; Yang, H.; Tang, Y.; Yi, Y.; Yao, W.; Wang, J.; Yi, Y. Broadband solar energy absorber based on monolayer molybdenum disulfide using tungsten elliptical arrays. *Mater. Today Energy* **2020**, *16*, 100390. [[CrossRef](#)]
9. Zhang, J.; Wang, H.; Yuan, X.; Zeng, G.; Tu, W.; Wang, S. Tailored indium sulfide-based materials for solar-energy conversion and utilization. *J. Photochem. Photobiol. C Photochem. Rev.* **2019**, *38*, 1–26. [[CrossRef](#)]
10. Alva, G.; Liu, L.; Huang, X.; Fang, G. Thermal energy storage materials and systems for solar energy applications. *Renew. Sustain. Energy Rev.* **2017**, *68*, 693–706. [[CrossRef](#)]
11. Marugán, A.P.; Márquez, F.P.G.; Perez, J.M.P.; Ruiz-Hernández, D. A survey of artificial neural network in wind energy systems. *Appl. Energy* **2018**, *228*, 1822–1836. [[CrossRef](#)]
12. Tascikaraoglu, A.; Uzunoglu, M. A review of combined approaches for prediction of short-term wind speed and power. *Renew. Sustain. Energy Rev.* **2014**, *34*, 243–254. [[CrossRef](#)]
13. Abe, J.O.; Popoola, A.P.I.; Ajenifuja, E.; Popoola, O.M. Hydrogen energy, economy and storage: Review and recommendation. *Int. J. Hydrogen Energy* **2019**, *44*, 15072–15086. [[CrossRef](#)]
14. Parra, D.; Valverde, L.; Pino, F.J.; Patel, M.K. A review on the role, cost and value of hydrogen energy systems for deep decarbonisation. *Renew. Sustain. Energy Rev.* **2019**, *101*, 279–294. [[CrossRef](#)]
15. Singh, D.; Sharma, D.; Soni, S.L.; Sharma, S.; Kumar Sharma, P.; Jhalani, A. A review on feedstocks, production processes, and yield for different generations of biodiesel. *Fuel* **2020**, *262*, 116553. [[CrossRef](#)]
16. Jahirul, M.I.; Koh, W.; Brown, R.J.; Senadeera, W.; O'Hara, I.; Moghaddam, L. Biodiesel production from non-edible beauty leaf (*Calophyllum inophyllum*) oil: Process optimization using response surface methodology (RSM). *Energies* **2014**, *7*, 5317–5331. [[CrossRef](#)]
17. Haseeb, A.S.M.A.; Fazal, M.A.; Jahirul, M.I.; Masjuki, H.H. Compatibility of automotive materials in biodiesel: A review. *Fuel* **2011**, *90*, 922–931. [[CrossRef](#)]
18. Rahman, M.M.; Pourkhesalian, A.M.; Jahirul, M.I.; Stevanovic, S.; Pham, P.X.; Wang, H.; Masri, A.R.; Brown, R.J.; Ristovski, Z.D. Particle emissions from biodiesels with different physical properties and chemical composition. *Fuel* **2014**, *134*, 201–208. [[CrossRef](#)]
19. Shi, W.; Li, J.; He, B.; Yan, F.; Cui, Z.; Wu, K.; Lin, L.; Qian, X.; Cheng, Y. Biodiesel production from waste chicken fat with low free fatty acids by an integrated catalytic process of composite membrane and sodium methoxide. *Bioresour. Technol.* **2013**, *139*, 316–322. [[CrossRef](#)]
20. Hoekman, S.K.; Broch, A.; Robbins, C.; Cenicerros, E.; Natarajan, M. Review of biodiesel composition, properties, and specifications. *Renew. Sustain. Energy Rev.* **2012**, *16*, 143–169. [[CrossRef](#)]
21. Jahirul, M.I.; Brown, R.J.; Senadeera, W.; O'Hara, I.M.; Ristovski, Z.D. The use of artificial neural networks for identifying sustainable biodiesel feedstocks. *Energies* **2013**, *6*, 3764–3806. [[CrossRef](#)]
22. Florin, M.J.; van Ittersum, M.K.; van de Ven, G.W.J. Selecting the sharpest tools to explore the food-feed-fuel debate: Sustainability assessment of family farmers producing food, feed and fuel in Brazil. *Ecol. Indic.* **2012**, *20*, 108–120. [[CrossRef](#)]
23. Babazadeh, R.; Razmi, J.; Pishvae, M.S.; Rabbani, M. A sustainable second-generation biodiesel supply chain network design problem under risk. *Omega* **2017**, *66*, 258–277. [[CrossRef](#)]
24. Bhuiya, M.M.K.; Rasul, M.G.; Khan, M.M.K.; Ashwath, N.; Azad, A.K.; Hazrat, M.A. Second Generation Biodiesel: Potential Alternative to-edible Oil-derived Biodiesel. *Energy Procedia* **2014**, *61*, 1969–1972. [[CrossRef](#)]
25. Anwar, M.; Rasul, M.G.; Ashwath, N. The efficacy of multiple-criteria design matrix for biodiesel feedstock selection. *Energy Convers. Manag.* **2019**, *198*, 111790. [[CrossRef](#)]
26. Sharma, R.; Gupta, A.; Abrol, G.S.; Joshi, V.K. Value addition of wild apricot fruits grown in north-west himalayan regions: A review. *J. Food Sci. Technol.* **2012**, *51*, 2917–2924. [[CrossRef](#)] [[PubMed](#)]
27. Kate, A.E.; Lohani, U.C.; Pandey, J.P.; Shahi, N.C.; Sarkar, A. Traditional and mechanical method of the oil extraction from wild apricot kernel: A comparative study. *Res. J. Chem. Environ. Sci.* **2014**, *2*, 54–60.
28. Wang, L.; Yu, H. Biodiesel from Siberian apricot (*Prunus sibirica* L.) seed kernel oil. *Bioresour. Technol.* **2012**, *112*, 355–358. [[CrossRef](#)]
29. Anwar, M.; Rasul, M.; Ashwath, N. Optimization of biodiesel production from stone fruit kernel oil. *Energy Procedia* **2019**, *160*, 268–276. [[CrossRef](#)]
30. Singh Gurau, V.; Agarwal, M.S.; Sarin, A.; Sandhu, S.S. Experimental Study on Storage and Oxidation Stability of Bitter Apricot Kernel Oil Biodiesel. *Energy Fuels* **2016**, *30*, 8377–8385. [[CrossRef](#)]
31. Gumus, M.; Kasifoglu, S. Performance and emission evaluation of a compression ignition engine using a biodiesel (apricot seed kernel oil methyl ester) and its blends with diesel fuel. *Biomass Bioenergy* **2010**, *34*, 134–139. [[CrossRef](#)]
32. Hanbey, H.; Mahmut, U.Y.A.R.; Aydin, H.; Emine, Ş.A.P. The effects of apricots seed oil biodiesel with some additives on performance and emissions of a diesel engine. *Int. J. Automot. Eng. Technol.* **2016**, *5*, 2146–9067.

33. Mullan Karishma, S.; Dasore, A.; Rajak, U.; Nath Verma, T.; Prahlada Rao, K.; Omprakash, B. Experimental examination of CI engine fueled with various blends of diesel-apricot oil at different engine operating conditions. *Mater. Today Proc.* **2021**, *49*, 307–310. [[CrossRef](#)]
34. Holman, J.P. *Experimental Methods for Engineers*, 7th ed.; Tata McGraw Hill: New Delhi, India, 2004.
35. Hasan, M.M.; Rahman, M.M. Performance and emission characteristics of biodiesel–diesel blend and environmental and economic impacts of biodiesel production: A review. *Renew. Sustain. Energy Rev.* **2017**, *74*, 938–948. [[CrossRef](#)]
36. Xue, J.; Grift, T.E.; Hansen, A.C. Effect of biodiesel on engine performances and emissions. *Renew. Sustain. Energy Rev.* **2011**, *15*, 1098–1116. [[CrossRef](#)]
37. Lin, B.-F.; Huang, J.-H.; Huang, D.-Y. Experimental study of the effects of vegetable oil methyl ester on DI diesel engine performance characteristics and pollutant emissions. *Fuel* **2009**, *88*, 1779–1785. [[CrossRef](#)]
38. Öner, C.; Altun, Ş. Biodiesel production from inedible animal tallow and an experimental investigation of its use as alternative fuel in a direct injection diesel engine. *Appl. Energy* **2009**, *86*, 2114–2120. [[CrossRef](#)]
39. Aydin, H.; Bayindir, H. Performance and emission analysis of cottonseed oil methyl ester in a diesel engine. *Renew. Energy* **2010**, *35*, 588–592. [[CrossRef](#)]
40. Utlu, Z.; Koçak, M.S. The effect of biodiesel fuel obtained from waste frying oil on direct injection diesel engine performance and exhaust emissions. *Renew. Energy* **2008**, *33*, 1936–1941. [[CrossRef](#)]
41. Anwar, M.; Rasul, M.; Ashwath, N.; Rahman, M. Optimisation of Second-Generation Biodiesel Production from Australian Native Stone Fruit Oil Using Response Surface Method. *Energies* **2018**, *11*, 2566. [[CrossRef](#)]
42. Benjumea, P.; Agudelo, J.R.; Agudelo, A.F. Effect of the Degree of Unsaturation of Biodiesel Fuels on Engine Performance, Combustion Characteristics, and Emissions. *Energy Fuels* **2011**, *25*, 77–85. [[CrossRef](#)]
43. Ozsezen, A.N.; Canakci, M.; Turkcan, A.; Sayin, C. Performance and combustion characteristics of a DI diesel engine fueled with waste palm oil and canola oil methyl esters. *Fuel* **2009**, *88*, 629–636. [[CrossRef](#)]
44. Nabi, M.N.; Rasul, M.G.; Anwar, M.; Mullins, B.J. Energy, exergy, performance, emission and combustion characteristics of diesel engine using new series of non-edible biodiesels. *Renew. Energy* **2019**, *140*, 647–657. [[CrossRef](#)]
45. Bhuiya, M.; Rasul, M.; Khan, M.; Ashwath, N. Performance and Emission Characteristics of Binary Mixture of Poppy and Waste Cooking Biodiesel. *Energy Procedia* **2017**, *110*, 523–528. [[CrossRef](#)]
46. Sanjid, A.; Kalam, M.A.; Masjuki, H.H.; Varman, M.; Zulkifli, N.W.B.M.; Abedin, M.J. Performance and emission of multi-cylinder diesel engine using biodiesel blends obtained from mixed inedible feedstocks. *J. Clean. Prod.* **2016**, *112*, 4114–4122. [[CrossRef](#)]
47. Rahman, M.M.; Rasul, M.G.; Hassan, N.M.S.; Azad, A.K.; Uddin, M.N. Effect of small proportion of butanol additive on the performance, emission, and combustion of Australian native first- and second-generation biodiesel in a diesel engine. *Environ. Sci. Pollut. Res. Int.* **2017**, *24*, 22402–22413. [[CrossRef](#)]
48. Anwar, M.; Rasul, M.G.; Ashwath, N. A comparative study of engine performance and emission characteristics of biodiesels produced from the waste seeds of papaya and stone fruit. In Proceedings of the 2019 IEEE 2nd International Conference on Renewable Energy and Power Engineering (REPE), Toronto, ON, Canada, 2–4 November 2019.
49. Anwar, M.; Rasul, M.; Ashwath, N. A Systematic Multivariate Analysis of Carica papaya Biodiesel Blends and Their Interactive Effect on Performance. *Energies* **2018**, *11*, 2931. [[CrossRef](#)]
50. Liaquat, A.M.; Masjuki, H.H.; Kalam, M.A.; Varman, M.; Hazrat, M.A.; Shahabuddin, M.; Mofijur, M. Application of blend fuels in a diesel engine. *Energy Procedia* **2012**, *14*, 1124–1133. [[CrossRef](#)]
51. Carraretto, C.; Macor, A.; Mirandola, A.; Stoppato, A.; Tonon, S. Biodiesel as alternative fuel: Experimental analysis and energetic evaluations. *Energy* **2004**, *29*, 2195–2211. [[CrossRef](#)]
52. Ong, H.C.; Masjuki, H.H.; Mahlia, T.M.I.; Silitonga, A.S.; Chong, W.T.; Leong, K.Y. Optimization of biodiesel production and engine performance from high free fatty acid Calophyllum inophyllum oil in CI diesel engine. *Energy Convers. Manag.* **2014**, *81*, 30–40. [[CrossRef](#)]
53. Mofijur, M.; Masjuki, H.H.; Kalam, M.A.; Atabani, A.E. Evaluation of biodiesel blending, engine performance and emissions characteristics of Jatropha curcas methyl ester: Malaysian perspective. *Energy* **2013**, *55*, 879–887. [[CrossRef](#)]
54. Qi, D.H.; Chen, H.; Geng, L.M.; Bian, Y.Z. Experimental studies on the combustion characteristics and performance of a direct injection engine fueled with biodiesel/diesel blends. *Energy Convers. Manag.* **2010**, *51*, 2985–2992. [[CrossRef](#)]
55. Anwar, M.; Rasul, M.G.; Ashwath, N. The synergistic effects of oxygenated additives on papaya biodiesel binary and ternary blends. *Fuel* **2019**, *256*, 115980. [[CrossRef](#)]
56. Sajjad, H.; Masjuki, H.; Varman, M.; Kalam, M.; Arbab, M.; Imtenan, S.; Ashraf, A. Influence of gas-to-liquid (GTL) fuel in the blends of Calophyllum inophyllum biodiesel and diesel: An analysis of combustion–performance–emission characteristics. *Energy Convers. Manag.* **2015**, *97*, 42–52. [[CrossRef](#)]
57. Mustayen, A.; Wang, X.; Rasul, M.; Hamilton, J.; Negnevitsky, M. Theoretical Investigation of Combustion and Performance Analysis of Diesel Engine under Low Load Conditions. In *IOP Conference Series: Earth and Environmental Science*; IOP Publishing: Bristol, UK, 2021.
58. Anwar, M.; Rasul, M.G.; Ashwath, N. Combustion characteristics of an agricultural diesel engine fuelled with papaya and stone fruit biodiesel: A comparison. In Proceedings of the 2019 IEEE 2nd International Conference on Renewable Energy and Power Engineering (REPE), Toronto, ON, Canada, 2–4 November 2019.

59. Ong, H.C.; Masjuki, H.H.; Mahlia, T.M.I.; Silitonga, A.S.; Chong, W.T.; Yusaf, T. Engine performance and emissions using *Jatropha curcas*, *Ceiba pentandra* and *Calophyllum inophyllum* biodiesel in a CI diesel engine. *Energy* **2014**, *69*, 427–445. [CrossRef]
60. Anwar, M.; Rasul, M.G.; Ashwath, N. Investigation on the impact of papaya biodiesel-diesel blends on combustion of an agricultural CI engine. *IOP Conf. Ser. Earth Environ. Sci.* **2020**, *463*, 012001. [CrossRef]
61. Devan, P.K.; Mahalakshmi, N.V. Performance, emission and combustion characteristics of poon oil and its diesel blends in a DI diesel engine. *Fuel* **2009**, *88*, 861–867. [CrossRef]
62. Godiganur, S.; Suryanarayana Murthy, C.; Reddy, R.P. Performance and emission characteristics of a Kirloskar HA394 diesel engine operated on fish oil methyl esters. *Renew. Energy* **2010**, *35*, 355–359. [CrossRef]
63. Anwar, M.; Rasul, M.G.; Ashwath, N. A pragmatic and critical analysis of engine emissions for biodiesel blended fuels. *Fuel* **2020**, *270*, 117513. [CrossRef]
64. Mustafa, E.T.; Van Gerpen, J.H.; Wang, P.S. Fuel Property Effects on Injection Timing, Ignition Timing, and Oxides of Nitrogen Emissions from Biodiesel-Fueled Engines. *Trans. ASAE* **2004**, *50*.
65. Yongcheng, H.; Longbao, Z.; Shangxue, W.; Shenghua, L. Study on the Performance and Emissions of a Compression Ignition Engine Fuelled with Fischer-Tropsch Diesel Fuel. *Proc. Inst. Mech. Eng. Part D J. Automob. Eng.* **2006**, *220*, 827–835. [CrossRef]
66. Fontaras, G.; Karavalakis, G.; Kousoulidou, M.; Tzamkiozis, T.; Ntziachristos, L.; Bakeas, E.; Stournas, S.; Samaras, Z. Effects of biodiesel on passenger car fuel consumption, regulated and non-regulated pollutant emissions over legislated and real-world driving cycles. *Fuel* **2009**, *88*, 1608–1617. [CrossRef]
67. Labeckas, G.; Slavinskas, S. The effect of rapeseed oil methyl ester on direct injection Diesel engine performance and exhaust emissions. *Energy Convers. Manag.* **2006**, *47*, 1954–1967. [CrossRef]
68. Qi, D.H.; Geng, L.M.; Chen, H.; Bian, Y.Z.; Liu, J.; Ren, X.C. Combustion and performance evaluation of a diesel engine fueled with biodiesel produced from soybean crude oil. *Renew. Energy* **2009**, *34*, 2706–2713. [CrossRef]
69. Keskin, A.; Gürü, M.; Altıparmak, D. Influence of tall oil biodiesel with Mg and Mo based fuel additives on diesel engine performance and emission. *Bioresour. Technol.* **2008**, *99*, 6434–6438. [CrossRef]
70. Gürü, M.; Koca, A.; Can, Ö.; Çınar, C.; Şahin, F. Biodiesel production from waste chicken fat based sources and evaluation with Mg based additive in a diesel engine. *Renew. Energy* **2010**, *35*, 637–643. [CrossRef]
71. Lin, C.-Y.; Li, R.-J. Engine performance and emission characteristics of marine fish-oil biodiesel produced from the discarded parts of marine fish. *Fuel Process. Technol.* **2009**, *90*, 883–888. [CrossRef]
72. Usta, N. An experimental study on performance and exhaust emissions of a diesel engine fuelled with tobacco seed oil methyl ester. *Energy Convers. Manag.* **2005**, *46*, 2373–2386. [CrossRef]
73. Koçak, M.S.; İleri, E.; Utlü, Z. Experimental Study of Emission Parameters of Biodiesel Fuels Obtained from Canola, Hazelnut, and Waste Cooking Oils. *Energy Fuels* **2007**, *21*, 3622–3626. [CrossRef]
74. Graboski, M.S.; McCormick, R.L.; Alleman, T.L.; Herring, A.M. The Effect of Biodiesel Composition on Engine Emissions from a DDC Series 60 Diesel Engine Final Report Report 2 in a Series of 6 National Renewable Energy Laboratory. 2003. Available online: <https://www.osti.gov/biblio/15003583-effect-biodiesel-composition-engine-emissions-from-ddc-series-diesel-engine-final-report-report-series> (accessed on 1 May 2019).
75. Monyem, A.; Gerpen, J.H.V.; Canakci, M. The effect of timing and oxidation on emissions from biodiesel-fueled engines. *Trans. ASABE* **2001**, *44*, 35–42. [CrossRef]
76. Abd-Alla, G.H.; Soliman, H.A.; Badr, O.A.; Abd-Rabbo, M.F. Effects of diluent admissions and intake air temperature in exhaust gas recirculation on the emissions of an indirect injection dual fuel engine. *Energy Convers. Manag.* **2001**, *42*, 1033–1045. [CrossRef]
77. Tse, H.; Leung, C.W.; Cheung, C.S. Investigation on the combustion characteristics and particulate emissions from a diesel engine fueled with diesel-biodiesel-ethanol blends. *Energy* **2015**, *83*, 343–350. [CrossRef]
78. Kaplan, C.; Arslan, R.; Sürmen, A. Performance Characteristics of Sunflower Methyl Esters as Biodiesel. *Energy Sources Part A Recovery Util. Environ. Eff.* **2006**, *28*, 751–755. [CrossRef]
79. Lin, L.; Cunshan, Z.; Vittayapadung, S.; Xiangqian, S.; Mingdong, D. Opportunities and challenges for biodiesel fuel. *Appl. Energy* **2011**, *88*, 1020–1031. [CrossRef]
80. Murillo, S.; Míguez, J.L.; Porteiro, J.; Granada, E.; Morán, J.C. Performance and exhaust emissions in the use of biodiesel in outboard diesel engines. *Fuel* **2007**, *86*, 1765–1771. [CrossRef]
81. Vijayaraj, K.; Sathiyagnanam, A.P.; Nagar, A. A Comprehensive Review on Combustion of Compression Ignition Engines Using Biodiesel. *IAEME* **2014**, *5*, 44–56.
82. Kale, T.P. Combustion of biodiesel in CI engine. *Int. J. Appl. Res.* **2017**, *3*, 145–149.
83. Agarwal, A.K.; Gupta, P.; Dhar, A. Combustion, performance and emissions characteristics of a newly developed CRDI single cylinder diesel engine. *Sadhana* **2015**, *40*, 1937–1954. [CrossRef]
84. Ryu, K. The characteristics of performance and exhaust emissions of a diesel engine using a biodiesel with antioxidants. *Bioresour. Technol.* **2010**, *101*, S78–S82. [CrossRef]
85. Tesfa, B.; Mishra, R.; Zhang, C.; Gu, F.; Ball, A.D. Combustion and performance characteristics of CI (compression ignition) engine running with biodiesel. *Energy* **2013**, *51*, 101–115. [CrossRef]
86. Sharma, N.; Agarwal, A.K. Effect of Fuel Injection Pressure and Engine Speed on Performance, Emissions, Combustion, and Particulate Investigations of Gasohols Fuelled Gasoline Direct Injection Engine. *J. Energy Resour. Technol.* **2019**, *142*, 042201. [CrossRef]

87. Najafi, B.; Pirouzpanah, V.; Ghobadian, B.; Sadeghpour Ranjbar, A. Experimental investigation of diesel engine performance parameters and pollution using biodiesel. *Modares Tech. Eng.* **2007**, *28*, 79–91.
88. Olalekan, W.S.; Rashid, A.A.; Dahlan, A. Combustion Characteristics of Spark Ignition Engine Fuelled by Compressed Natural Gas in a Direct Injection Compressed Natural Gas Engine. *Int. J. Appl. Eng. Res.* **2018**, *13*, 727–731.
89. Prashant, G.K.; Lata, D.B.; Joshi, P.C. Investigations on the effect of methanol blend on the combustion parameters of dual fuel diesel engine. *Appl. Therm. Eng.* **2016**, *103*, 187–194. [[CrossRef](#)]